A Simple Manifold-Based Construction of Surfaces of Arbitrary Smoothness

Lexing Ying, Denis Zorin
New York University

Abstract

We present a smooth surface construction based on the manifold approach of Grimm and Hughes. We demonstrate how this approach can relatively easily produce a number of desirable properties which are hard to achieve simultaneously with polynomial patches, subdivision or variational surfaces. Our surfaces are C^∞-continuous with explicit nonsingular C^∞ parameterizations, high-order flexible at control vertices, depend linearly on control points, have fixed-size local support for basis functions, and have good visual quality.

CR Categories: I.3.5 Computational Geometry and Object Modeling; Curve, surface, solid, and object representations

Keywords: Geometric modeling, manifolds.

1 Introduction

Much of the work on smooth surface representations, excluding variational surfaces, is based on the paradigm of stitching polynomial patches together. While subdivision surfaces are generally defined as limits of recursive refinement algorithms, the surfaces produced by most popular schemes can still be interpreted as infinite collections of stitched spline patches.

In this paper we take a different, often neglected approach based on the manifold construction of [Grimm and Hughes 1995]. We demonstrate how this approach can produce with relative ease a number of desirable properties which are hard to achieve simultaneously with polynomial patches, subdivision or variational surfaces. Specifically, our surfaces have the following properties:

- *Any prescribed degree of smoothness including C^∞ with explicit nonsingular parameterizations of the same smoothness.* It is widely recognized that C^2-continuity is important for visual quality, as it insures smooth normal variation. Higher degrees of smoothness are useful for numerical purposes: for example, for C^3-continuous surfaces variation of curvature functionals are well-defined everywhere, C^k-continuity makes it possible to use high-order quadratures to ensure rapid convergence (theoretically at super-algebraic rates for C^∞-surfaces). Explicit closed-form parameterizations are always preferable for a variety of tasks, from texturing to surface-surface intersections.
- *The surfaces are at least 3-flexible.* i.e. can have arbitrary prescribed derivatives of order up to three at control vertices. This property ensures that a surface does not have artificial flat spots.
- *Linear dependence on control points, fixed-size local support for basis functions.* Linear dependence on control points considerably simplifies formulation of a number of algorithms, e.g. surface fitting. Localized influence of control points is important both for efficiency and intuitive surface control.
- *Good visual quality.* Many surfaces constructed to precise mathematical specifications often suffer from inferior surface quality. We demonstrate how good visual surface quality can be achieved simultaneously with many useful mathematical properties.

Apart from making this combination of desirable qualities possible, manifold representations are useful for a number of reasons. For example, this is a natural setting for *solving equations on surfaces* (e.g. reaction-diffusion or fluid flow [Stam 2003]) as the chart overlap simplifies maintaining smoothness of solutions across boundaries. For manifolds it is easier *to apply algorithms designed for parametric patches* which treat the surface as a function $f(u, v)$ to surfaces of arbitrary topology without handling special cases for inter-patch boundaries needed for patch-based representations. If one needs *to define a hierarchical basis on a manifold surface*, one can simply define it on the plane and then use the chart parametrization to transfer it to the surface. Such bases can be used in many contexts requiring approximation: fitting, trimming, boolean operations etc.

Our work was initially motivated by the needs of a specific application in scientific computing: boundary integral equations on surfaces, which, in graphics literature have appeared in [James and Pai 1999]. Our application required high-order smooth nonsingular parametrization to ensure fast convergence of quadrature rules on surfaces, i.e. for the parametrization to have good *mathematical quality*; at the same time, it was essential to be able to model objects of arbitrary shape and obtain good *visual quality* without additional processing.

We have observed that even all existing flexible C^2 constructions are quite complex, and while higher-order constructions exist, despite having nice mathematical properties, few were ever fully implemented and visual surface quality was typically inferior to lower-order schemes. Subdivision surfaces are a notable exception: they were not constructed to satisfy a specific set of requirements. Rather, it was observed that the subdivision algorithms for splines generalize well to arbitrary control meshes, and the visual quality of the surface is adequate in an intuitive sense, except for high-valence vertices. Analysis of properties came later and is quite complex. Even obtaining a C^1 nonsingular parametrization is nontrivial and requires inversion of the characteristic map [Stam 1998].

In our approach, we relax the requirement of representing surfaces using polynomial patches to simplify the construction needed to achieve good mathematical quality, and we ensure that our surfaces closely approximate the shape of subdivision surfaces to achieve acceptable visual quality for a similar range of vertex valences.

We believe that due to the properties enumerated above, manifold representations provide the most convenient basis for "black-box" surface approximation software: the user provides an input control mesh, and the surface and its parametric derivatives of any order can be evaluated at any point. While the black-box approach is not the most efficient, it is the most convenient and reliable one for applications requiring a large variety of algorithms to operate on surfaces.

Acknowledgments. We would like to thank Elif Tosun for her help with the project and the anonymous reviewers for many useful comments. This research was supported in part by NSF awards DMS-9980069, CCR-0093390, and CCR-9988528, Sloan Foundation Fellowship, IBM University Partnership Award and NYU Dean's Dissertation Fellowship.

2 Previous work

We are not aware of any C^∞ constructions for surfaces with general control meshes.

The work on computational representations of surfaces based on manifolds is relatively limited. The idea was introduced in [Grimm and Hughes 1995]. More recently, [Navau and Garcia 2000] have proposed a C^k construction based only on polynomials. Parameterization techniques using the manifolds can also be found in [Grimm 2002] and [Grimm and Hughes 2003].

Extensive literature exists on spline-based constructions of different types; C^k constructions include S-patches [Loop and DeRose 1989], DMS splines [Seidel 1994], freeform splines [Prautzsch 1997] and TURBS [Reif 1998]. DMS splines were developed to the greatest extent; as a large number of knots and control points need to be introduced for each triangle, an additional algorithm is needed to position these points if only an initial mesh is given. TURBS are based on singular parameterizations; for both free-form splines and TURBS additional degrees need to be set, which can be done using fairing functionals and precomputed matrices, similar to the technique that we use. There are numerous C^2 constructions, e.g. [Gregory and Hahn 1989], [Wang 1992], [Peters 1996], [Hermann 1996], [Bohl and Reif 1997], and most recently [Peters 2002]. There is an even larger number of C^1-constructions; excluding subdivision surfaces, which are C^2 away from isolated points, these constructions rarely yield surfaces of acceptable quality. In all cases, the required polynomial degree and number of additional patch control points to be set rapidly grows with smoothness.

Unfortunately, in most cases it is impossible to compare the visual quality of resulting surfaces to our construction. The implementation is complex, and only few images of simple objects are provided in the papers, as the stated goal in most cases is to obtain surfaces satisfying a specific mathematical condition.

The literature related to subdivision surfaces is extensively reviewed in the book [Warren and Weimer 2001] and in the course notes [Zorin et al. 2001]. Direct fixed-time evaluation of subdivision surfaces was introduced in [Stam 1998], which is the only known approach to directly cast subdivision surfaces in parametric form. [Peters 2000] describes a technique for approximating Catmull-Clark surfaces with a collection of bicubic patches joined with C^1 continuity.

3 Construction

Manifold structure. We consider meshes consisting of quadrilaterals, although this is not critical for our construction: it can be carried out in a similar way using triangle meshes and Loop subdivision surfaces, for example. We focus on the quadrilateral case as it has more relevance for geometric modeling applications.

The foundation of our approach is a simple construction of a C^∞-manifold associated with a mesh. We refer the reader for detailed discussion of manifolds to [Grimm and Hughes 1995]. Here we just state the basic definition: a set M has 2D manifold structure, if a collection of charts (C_i, φ_i) is defined, where C_i are open domains in the plane, φ_i are one-to-one maps $C_i \to M$, such that the images $\varphi_i(C_i)$ cover all of M[1]. M is a C^∞ manifold if the transition maps from chart to chart $t_{ji} = \varphi_j^{-1} \circ \varphi_i$ defined for pairs of chart for which $\varphi_i(C_i)$ and $\varphi_j(C_j)$ intersect, are C^∞. In our construction, we use the control mesh as the domain M[2].

Another important idea that we use is the *partition of unity*. A set of functions w_i each defined on C_i, and having compact support, is called a partition of unity, if $\sum_i w_i \circ \varphi_i^{-1} = 1$, where the summation is over all charts.

Overview of the construction. The general approach is close to the one in [Grimm and Hughes 1995]. We construct functions $f_i^l : C_i \to \mathbf{R}^3$, defining the geometry locally on each chart; then, we use a partition of unity to define the global geometry. On M, the complete surface is defined by $\sum_i (w_i f_i^l) \circ \varphi_i^{-1}$. However, in practice it is evaluated on individual charts C_i via

$$f_i(x) = \sum_{j:\varphi_i(x)\in\varphi_j(C_j)} w_j(t_{ji}(x)) f_j^l(t_{ji}(x)) \qquad (1)$$

Note the complexity of evaluation of this expression is determined by three factors: complexity of transition maps t_{ij}, weights w_j and geometry functions f_j^l. In our case, the transition maps can be expressed in complex form as z^α (up to a rotation), the weights are piecewise exponential and C^∞, and the geometry functions are polynomials of degrees proportional to the valence of vertices corresponding to the charts.

Another important observation is that every $f_i(x)$ is C^∞ if all components are C^∞. Next, we discuss each component separately.

Charts and transition maps. As a basis for our construction, we use the conformal atlas for meshes. Conformal atlas has already been used in several graphics applications, most recently in [Gu and Yau 2003]. While many variations can be found in the literature (e.g. [Duchamp et al. 1997] in the context of parametrization), a complete description of the specific structure is not easily available, and we present it here. We define charts per vertex. Each chart domain is a curved star shape D_i, shown in Figure 1. The overlap region between the images of two charts in the control mesh is two faces of the mesh. Rather than constructing the maps φ_i, we construct the maps φ_i^{-1}. The chart construction proceeds in two steps: first, the faces adjacent to a given vertex are mapped piecewise bilinearly to the plane (maps L_i to domains S_i). Then a transformation c_i is applied to each wedge of the regular star S_i; c_i squeezes it so that it becomes a conformal image of square. Maps c_i have simple explicit expressions for each wedge. As illustrated in Figure 2 for the shown choice of coordinate system, these maps are compositions of a linear map l_{k_i} defined as matrix $diag(\cos(\pi/4)/\cos(\pi/k_i), \sin(\pi/4)/\sin(\pi/k_i))$, where k_i is the valence of D_i and a simple map g_{k_i}, which using standard identification of the plane with complex numbers $z = x + iy$, can be written as z^{4/k_i}. The chart maps φ_i^{-1} are compositions $c_i \circ L_i$.

This atlas has an important property: *all transition maps are conformal, in particular, C^∞*. In fact, the transition maps, for a certain choice of the coordinate systems can be written as z^{k_1/k_2}. This is proved in Appendix A. The fact that transition maps have simple expressions is very important; it allows us to define the geometry in an efficiently computable way. We can also replace z^{4/k_i} with more general functions of the form $|z|^p (z/|z|)^{4/k_i}$ for $p > 0$, which are

[1] In our definition, the charts are maps from 2D domains to the manifold, i.e. are inverses of chart maps defined in most differential geometry books. We use the nonstandard definition to simplify notation.

[2] For this we need to assume that the mesh has no self-intersections. This assumption is not crucial (we can construct the domain in a more abstract manner) but simplifies explanations. It has no implications for implementation.

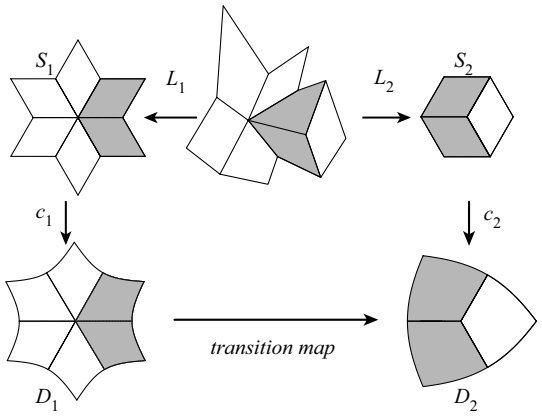

Figure 1: Construction of the charts. The maps L_i, $i = 1, 2$ are piecewise bilinear; the maps c_i are constructed on individual wedges as shown in Figure 2.

Figure 2: On each wedge, the map c_i is a composition of a linear map and the map z^{4/k_i}.

again C^∞-continuous. In the examples in Section 4, we choose $p = \log_2(1/\lambda_{k_i})$ where λ_{k_i} is the second largest eigenvalue of the Catmull-Clark subdivision matrix at valence k_i, to improve the quality of the geometry fit described below.

Partition of unity. The partition of unity is a crucial element of our construction: the quality of surface is defined not only by the quality of the geometry functions but also by how well they are blended. Our empirical observations are that it cannot have transition regions which are too steep, and, even more importantly, its support shape should match the shape of the star-like shape of the corresponding chart.

We build the partition of unity from identical pieces defined initially on the standard square $[0, 1]$ as a product of two identical one-dimensional functions $\eta(u)\eta(v)$. The function η is defined as follows [Bruno and Kunyansky 2001]:

$$\eta(t) = \begin{cases} 1 & : 0 \le t \le \delta \\ \frac{h((t-\delta)/a)}{h((t-\delta)/a)+h(1-(t-\delta)/a)} & : \delta < t < 1-\delta \\ 0 & : 1-\delta \le t \le 1 \end{cases}$$

where $\delta > 0$, $a = 1 - 2\delta$ and $h(s) = \exp(2\exp(-1/s)/(s-1))$. The resulting function is quite close in appearance to a Hermite spline (Figure 3). We set $\delta > 0$ for the following reason: When

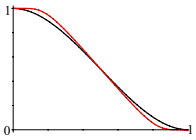

Figure 3: Red: the function $\eta(t)$ used in the construction of the partition of unity. Black: a Hermite spline which is close to the shape of $\eta(t)$.

$\delta = 0$, the transition maps has unbounded derivatives at the boundary of the overlapping charts. While it is possible that the composition of the transition map and the partition of unity has bounded derivatives if the partition of unity has sufficiently fast decay, we simply choose the partition of unity to be constant near the boundary. In our implementation, we use $\delta = 1/8$.

Once the function is defined on the square, we obtain a weight, defined on the whole chart as follows. First, we use a rotation by $\pi/4$ combined with the map $g_k^{-1} = z^{k/4}$ to remap $\eta(u)\eta(v)$ to a single wedge. The function is defined by rotational symmetry on the rest of the chart. *The resulting function is C^∞ on the whole chart.* The proof is outlined in Appendix A.

If only C^k surfaces for some finite k are desired, a suitably spline function of degree $k + 1$ can be used instead of $\eta(t)$.

Defining geometry. We define geometry using polynomials. The basic idea is to apply several subdivision steps to define the overall coarse shape of the surface, and use polynomials in the chart to fit this shape in the least square sense. As the fit is linear and the control points of refined subdivision mesh depend linearly on the control points of the original mesh, the transformation matrix converting control points to the polynomial coefficients can be precomputed. Thus, in practice the process is reduced to assembling a vector of control points and multiplying them by a matrix.

Every control point of the refined mesh after two Catmull-Clark subdivision steps can be assigned to the points with bilinear coordinates $(i/4, j/4)$ in each sector of the star S_k. For each vertex v, we remap these points in S_k to the chart domain D_k by using the map c_i. There are $m = 12k + 1$ points *inside* D_k which we denote $x_0, \dots x_{m-1}$. We compute 3D limit positions for these points in the same order, and denote them $s_0, \dots, s_{m-1}$. Our goal is to define a geometry function f such that differences $f(x_i) - s_i$ are minimized in the least squares sense.

In the fitting process, we use the monomials of total degree $\le d = \lfloor \mathbf{min}(14, k + 1) \rfloor$ as the basis functions. The choice of 14 as the maximal degree is empirical: using higher-order polynomials results in lower quality surfaces for high valences. We denote these monomials $p_0, \dots, p_{n-1}$ where $n = (d+1)(d+2)/2$ is the number of monomials used in the fitting. We use the least square fit to solve for the basis coefficients a_j, such that $f = \sum_{j=0}^{n-1} a_j p_j$. Let a be the vector of coefficients a_j, s be the vector of values s_i and U be the $m \times n$ matrix of monomial values $p_j(x_i)$ at points x_i. Then the least squares fit minimizing $\|Ua - s\|^2$ is given by

$$a = U^+ s$$

where $(\cdot)^+$ denotes pseudoinverse. The $n \times m$ matrix U^+ only depends on the valence k since x_i and p_j depend only on k. Therefore, it can be precomputed once and used for all charts with the same valence.

Flexibility of the surface at vertices in the center of the charts is easy to show, as one can construct specific control point configurations yielding various low-degree polynomials in a direct form.

We note that the above construction is the simplest among those we have tried; its disadvantage is the relatively large size of U_k, which can be reduced by using a more careful choice of polynomial bases and the singular value decomposition (SVD) from n to $3k+1$ without loosing surface quality.

If only C^k smoothness is needed, one can use tensor-product splines of fixed bidegree $k + 1$ instead of polynomials; the nature of the fitting process does not change.

4 Results

Implementing our scheme is relatively simple: our basic implementation has 1,500 lines of code including subdivision but excluding

SVD code. Most images in Figures 4 and 6 have a reflection map on a part of the surface to show the surface quality.

Figure 4 shows the quality of the surface generated by our method. On the left is a detailed comparison of the surfaces with Catmull-Clark surfaces near valence 5, 8 and 12 vertices. The quality is close, except in the immediate neighborhood of the vertex, where reflection lines show lack of C^2-continuity of Catmull-Clark. On the right, we present the plots for the principal curvature directions and Gaussian and mean curvatures.

Figure 5 shows the chart parameterization of our surfaces. On the left, a uniformly spaced checkerboard demonstrates that our surface parameterization is smooth at the extraordinary vertex, while the natural parameterization of Catmull-Clark surface is singular there. On the right, we show the sum of the magnitudes of the derivatives of the parametrization on a chart, to demonstrate the variation. We note that starting from fourth derivatives the behavior is dominated by the behavior of the derivatives of the partition of unity functions.

Figure 6 shows several examples of surfaces obtained from various control meshes. In all cases, overall quality is quite similar to Catmull-Clark surfaces; as expected, with smoother reflection lines near extraordinary vertices as in Figure 4.

Conclusions and Future Work The development of the construction described in this paper was initially driven by specific needs of an application, and it nicely meets its needs while being a completely general tool. We have no doubts that our construction can be improved in a variety of ways, as most of the components were identified empirically: in particular, to get good behavior of higher order derivatives, one needs a better partition of unity. It is quite possible that there are better charts, fewer or lower degree polynomials can be used for geometric functions, or entirely different geometric functions yield better results.

It is one of the many possible high-smoothness constructions of this type. We hope it will inspire future work in similar directions; as it is demonstrated by our construction, some problems which are difficult or impossible to solve in a conventional framework can be resolved much more easily using alternative approaches.

A Proof of C^∞ continuity of transition maps and partition of unity functions.

Transition maps. Let us fix coordinate systems in the domains S_i, $i = 1, 2$ depicted in Figure 1 with x direction along the common edge of two shaded wedges. Let L_i', $i = 1, 2$ be the piecewise linear maps from a pair of adjacent unit squares. We also assume the coordinate system x axis to be along the common edge. A similar choice is made for domains D_i. The maps c_i for these coordinates can be written as $R(\pi/k_i)g_{k_i}l_{k_i}R(-\pi/k_i)$ for the top quad and $R(\pi/k_i)g_{k_i}l_{k_i}R(-\pi/k_i)$, where k_i is the valence of the corresponding vertex, $R(\alpha)$ is the rotation by the angle α, and the maps l_{k_i} and g_{k_i} are defined in Section 3.

The transition map $c_2L_2L_1^{-1}c_1^{-1}$ can then be written as $c_2L_2'L_1'^{-1}c_1^{-1}$, with the mesh maps itself eliminated. This can be done, as the composition of a linear and a bilinear map is bilinear, and the maps are defined uniquely by the correspondence of the domain corners, $L_i = L_i'L$, so the bilinear part L is factored out.

Next, we observe that the two piecewise linear parts of L_i' are just $R(\pi/k_i)l_{k_i}^{-1}R(-\pi/4)$ and $R(-\pi/k_i)l_{k_i}^{-1}R(\pi/4)$ in the chosen coordinate system.

Therefore, the transition map can be rewritten, say, on the top square as $R(\pi/k_2)g_{k_2}g_{k_1}^{-1}R(-\pi/k_1)$. In the complex form, the rotation is just a multiplication by $\exp(i\alpha)$. the transition map is $(\exp(-i\pi/k_1)z)^{k_1/k_2}\exp(i\pi/k_2) = z^{k_1/k_2}$. Exactly the same can be shown for the bottom square.

Partition of unity functions. One can easily verify that derivatives of all orders of $\eta(u)\eta(v)$, defined in Section 3 involving v, are zero at the boundary $v = 0$, and same is true for $u = 0$ by symmetry. Remapping to a wedge using a non-degenerate C^∞ map does not change the fact that all derivatives vanish identically, except derivatives along the boundary; the map that we use may not be differentiable at zero, but in a neighborhood of zero the function $\eta(u)\eta(v)$ is constant. By symmetry, these match at all orders after rotations extending the map to all wedges.

References

BOHL, H., AND REIF, U. 1997. Degenerate Bézier patches with continuous curvature. *Comput. Aided Geom. Design 14*, 8, 749–761.

BRUNO, O. P., AND KUNYANSKY, L. A. 2001. A fast, high-order algorithm for the solution of surface scattering problems: basic implementation, tests, and applications. *J. Comput. Phys. 169*, 1, 80–110.

DUCHAMP, T., CERTAIN, A., DEROSE, A., AND STUETZLE, W. 1997. Hierarchical computation of pl harmonic embeddings. Tech. rep., University of Washington.

GREGORY, J. A., AND HAHN, J. M. 1989. A $C\mathrm{span}2$ polygonal surface patch. *Comput. Aided Geom. Design 6*, 1, 69–75.

GRIMM, C. M., AND HUGHES, J. F. 1995. Modeling surfaces of arbitrary topology using manifolds. In *Proceedings of SIGGRAPH 95*, Computer Graphics Proceedings, Annual Conference Series, 359–368.

GRIMM, C. M., AND HUGHES, J. F. 2003. Parameterizating n-holed tori. In *The Mathematics of Surfaces IX*.

GRIMM, C. M. 2002. Simple manifolds for surface modeling and parameterization. In *Shape Modeling International*.

GU, X., AND YAU, S.-T. 2003. Global conformal surface parameterization. In *Proceedings of the Eurographics/ACM SIGGRAPH symposium on Geometry processing*, Eurographics Association, 127–137.

HERMANN, T. 1996. G^2 interpolation of free form curve networks by biquintic Gregory patches. *Comput. Aided Geom. Design 13*, 9, 873–893. In memory of John Gregory.

JAMES, D. L., AND PAI, D. K. 1999. Artdefo: accurate real time deformable objects. In *Proceedings of the 26th annual conference on Computer graphics and interactive techniques*, ACM Press/Addison-Wesley Publishing Co., 65–72.

LOOP, C. T., AND DEROSE, T. D. 1989. A multisided generalization of bézier surfaces. *ACM Trans. Graph. 8*, 3, 204–234.

NAVAU, J. C., AND GARCIA, N. P. 2000. Modeling surfaces from meshes of arbitrary topology. *Comput. Aided Geom. Design 17*, 7, 643–671.

PETERS, J. 1996. Curvature continuous spline surfaces over irregular meshes. *Comput. Aided Geom. Design 13*, 2, 101–131.

PETERS, J. 2000. Patching Catmull-Clark meshes. In *Proceedings of ACM SIGGRAPH 2000*, Computer Graphics Proceedings, Annual Conference Series, 255–258.

PETERS, J. 2002. C^2 free-form surfaces of degree $(3, 5)$. *Comput. Aided Geom. Design 19*, 2, 113–126.

PRAUTZSCH, H. 1997. Freeform splines. *Comput. Aided Geom. Design 14*, 3, 201–206.

REIF, U. 1998. TURBS—topologically unrestricted rational B-splines. *Constr. Approx. 14*, 1, 57–77.

SEIDEL, H.-P. 1994. Polar forms and triangular B-Spline surfaces. In *Euclidean Geometry and Computers, 2nd Edition*, D.-Z. Du and F. Hwang, Eds. World Scientific Publishing Co., 235–286.

STAM, J. 1998. Exact evaluation of Catmull-Clark subdivision surfaces at arbitrary parameter values. In *Proceedings of SIGGRAPH 98*, ACM SIGGRAPH / Addison Wesley, Orlando, Florida, Computer Graphics Proceedings, Annual Conference Series, 395–404. ISBN 0-89791-999-8.

STAM, J. 2003. Flows on surfaces of arbitrary topology. *ACM Trans. Graph. 22*, 3, 724–731.

WANG, T. J. 1992. A C^2-quintic spline interpolation scheme on triangulation. *Comput. Aided Geom. Design 9*, 5, 379–386.

WARREN, J., AND WEIMER, H. 2001. *Subdivision Methods for Geometric Design*. Morgan Kaufmann.

ZORIN, D., SCHRÖDER, P., DEROSE, A., KOBBELT, L., LEVIN, A., AND SWELDENS., W., 2001. Subdivision for modeling and animation. SIGGRAPH 2001 Course Notes.

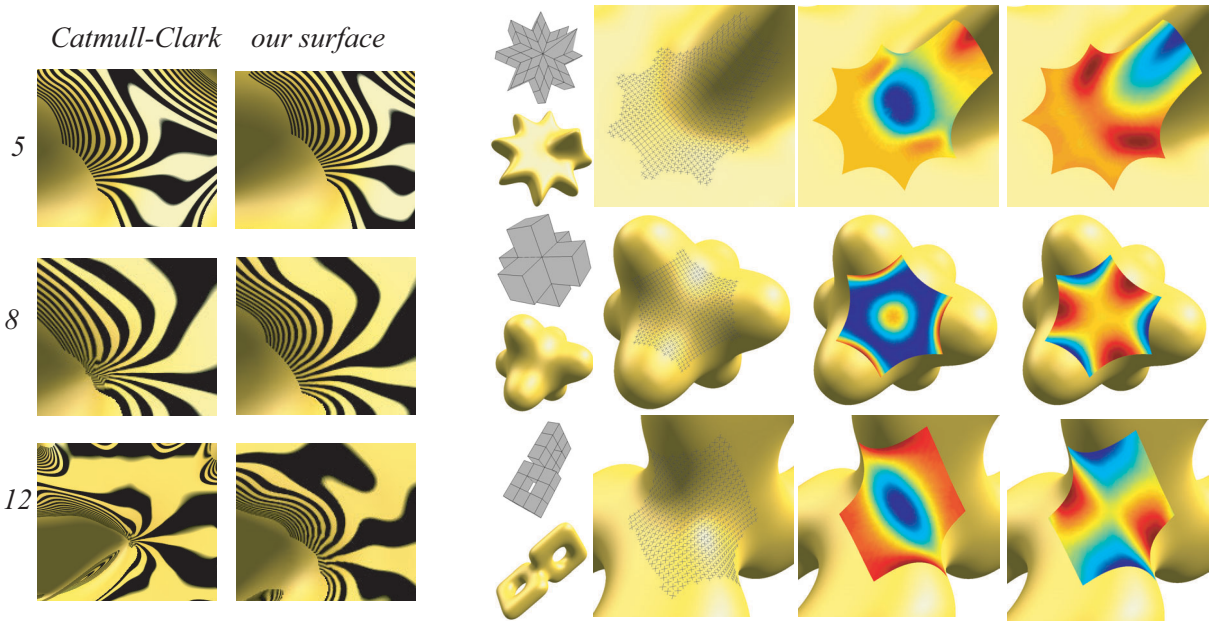

Figure 4: Left: comparison of surface behavior near extraordinary points for valence 5, 8 and 12. Right: principal curvature directions, Gaussian curvature and mean curvature around extraordinary vertices.

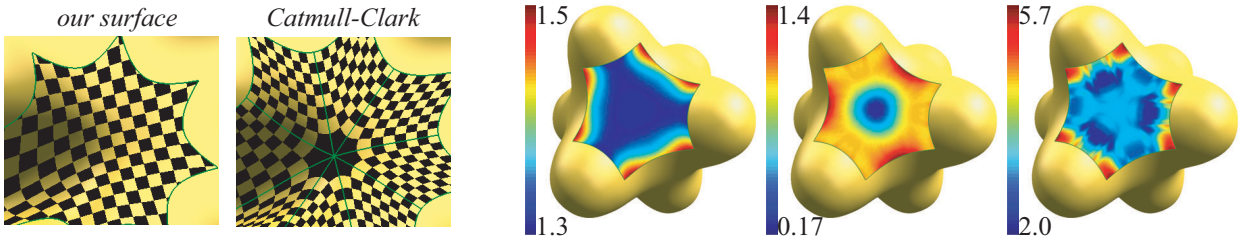

Figure 5: Left: comparison of parameterization. Right: maps of the total derivative magnitudes under our parameterization for the first, second and third derivatives.

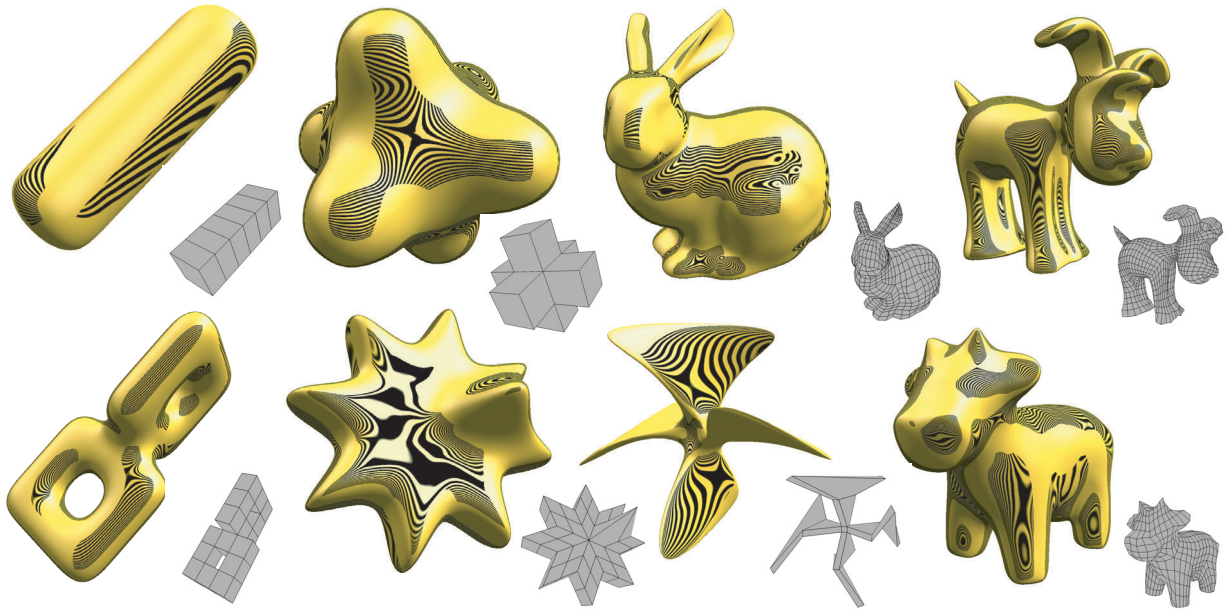

Figure 6: Several examples of the surfaces produced by our method.